Efficient top-emitting white organic light emitting device with an extremely stable chromaticity and viewing-angle*

Shao Ming(邵 茗), Guo Xu(郭 旭), Chen Shu-Fen(陈淑芬)†,
Fan Qu-Li(范曲立), and Huang Wei(黄 维)‡

Key Laboratory Cultivation Base for Organic Electronics and Information Displays and Institute of Advanced Materials, Nanjing University of Posts and Telecommunications, Nanjing 210046, *China*

(Received 13 February 2012; revised manuscript received 16 April 2012)

In this paper, we report on the fabrication of a top-emitting electrophosphorescent p–i–n white organic light-emitting diode on the basis of a low-reflectivity Sm/Ag semi-transparent cathode together with a thickness-optimized ZnS out-coupling layer. With a 24-nm out-coupling layer, the reflectivity of the cathode is reduced to 8% at 492 nm and the mean reflectivity is 24% in the visible area. By introducing an efficient electron blocking layer tris(1-phenylpyrazolato,N,C2′)iridium(III) ($Ir(ppz)_3$) to confine the exciton recombination area, the current efficiency and the colour stability of the device are effectively improved. A white emission with the $Ir(ppz)_3$ layer exhibits a maximum current efficiency of 9.8 cd/A at 8 V, and the Commission Internationale de L'Eclairage (CIE) chromaticity coordinates are almost constant during a large voltage change of 6 V–11 V. There is almost no viewing angular dependence in the spectrum when the viewing angle is no more than 45°, with a $CIE_{x,y}$ coordinate variation of only (±0.0025, ±0.0008). Even at a large viewing angle (75°), the $CIE_{x,y}$ coordinate change is as small as (±0.0087, ±0.0013).

Keywords: white organic light-emitting diode, top-emitting, electron blocking layer, high efficiency, colour stability

PACS: 85.60.Jb, 78.60.Fi, 81.05.Fb **DOI:** 10.1088/1674-1056/21/10/108507

1. Introduction

White organic light-emitting devices (WOLEDs) have attracted more and more attention in recent years because of their potential application in flat-panel displays, solid-state lighting, and liquid-crystal display backlighting sources.[1−3] These applications require WOLED to possess high brightness, high efficiency, and a long lifetime. For lighting purposes, some characterization parameters, such as the Commission Internationale de L'Eclairage (CIE) chromaticity coordinates of a near white light equal-energy point (0.33, 0.33), a colour temperature between 3000 K and 7500 K, and a colour-rendering index of above 80 are necessary for obtaining a high-quality white emission. In addition, colour stability is a primary concern in WOLED for both display and lighting applications since the shift in colour with the bias/current/luminance will bring some visual alterations to the human eye.

Unfortunately, many WOLEDs show variation in colour with bias voltage or current, regardless of their structure, whether single-layer or multilayer. This bias or current dependence may result from different factors in such devices with different structures, which have been investigated by many researchers in the past decade.[4−14]

The change of exciton recombination zones is a

*Project supported by the Science Fund of the Ministry of Science and Technology, China (Grant No. 2009CB930600), the National Natural Science Foundation of China (Grants Nos. 60907047, 61274065, and 60977024), the Key Project of the Chinese Ministry of Education (Grants Nos. 104246 and 707032), the Research Fund for the Doctoral Program of Higher Education Institutions, China (Grant Nos. 20093223120003 and 20093223110003), the Natural Science Foundation of Jiangsu Province and the Higher Education Institutions of Jiangsu Province, China (Grants Nos. BK2009423, SJ209003, 10KJB510013, and 11KJD510003), the Fok Ying-Tong Education Foundation, China (Grant No. 111051), the "Qing Lan" Program of Jiangsu Province and the "Pandeng" Project of Nanjing University of Posts and Telecommunications, China (Grant Nos. NY210015, NY211069, and NY210040).

†Corresponding author. E-mail: iamsfchen@njupt.edu.cn

‡Corresponding author. E-mail: wei-huang@njupt.edu.cn

© 2012 Chinese Physical Society and IOP Publishing Ltd

major problem that results in the variation of CIE coordinates in multi-emitting layer WOLEDs. Therefore, an effective control of the location of the exciton recombination zone is critical for obtaining a stable electroluminescence (EL) spectrum. WOLED with a charge confining structure without an interlayer has been proposed to simplify the fabrication process and achieve a high colour stability. However, most of reports focused on a bottom-emitting WOLED, so it is desirable to develop a top-emitting WOLED (TWOLED) since it not only can be fabricated on an opaque and flexible subatrate, such as metal foils, but also can provide a high-aperture ratio and a high resolution. However, the highly reflective metal is commonly used as both a cathode and anode, so the microcavity effect exits inevitably in TWOLED.[15] The full width at half maximum of the outcoupled emission spectrum is narrow, which leads to a challenge in requiring the broadband emission of white light. These drawbacks can be overcome by applying an additional dielectric organic layer on the top of the TWOLED. This increases the transmittance through the top electrode, reduces the microcavity effect, and alleviates the viewing angle dependence.

In this paper, we report on a new TWOLED structure combining a p–i–n structure with a dual emitting layer (EML) of red and blue to synthesize the white emission. The red and blue dopants reported here are iridium(III)bis(2-methyldibenzo-[f,h]quinoxaline)(acetylacetonate) ($Ir(MDQ)_2(acac)$) and iridium(III)bis[4,6-(di-fluorophenyl)-pyridinato-N,$C^{2\prime}$] picolinate (FIrpic), respectively. At the same time, a high triplet energy host material,[16] 9,9-spirobifluroren-2-yl-diphenyl-phoaphine oxide (SPPO1), is used as the blue host. By using a p–i–n structure, the operating voltage can be considerably reduced in the TWOLED. The highly conductive p- and n-doped layers can enhance the charge injection from the contacts and reduce the Ohmic losses in these layers. The p- and n-dopants reported here are tetrafluoro-tetracyanoqino dimethane (F_4-TCNQ) and Li, respectively. The strategy of inserting an electron blocking layer to control the recombination zone in the TWOLED is shown to be effective in improving performance including realizing a lower leakage current, a lower turn-on voltage, a higher luminance, and optical stability at a high current density.

2. Experiment

The detailed device structures used in this paper are listed in Table 1. Here, F4-TCNQ doped N, N, N′, N′-tetrakis(4-methoxyphenyl)-benzidine (MEO-TPD) and Li doped 4,7-diphenyl-1,10-phenanthroline (Bphen) are used as the p-doped transport layer (p-HTL) and n-doped transport layer (n-ETL), respectively. In device A, MEO-TPD, (4,4′-N,N′-dicarbazole)biphenyl (CBP), $Ir(MDQ)_2(acac)$, SPPO1, FIrpic, and Bphen are utilized as a hole transport layer, a red host, a red phosphorescent guest, a blue host, a blue phosphorescent guest and an electron transport layer, respectively. Device B employs two EMLs sandwiched between the blocking materials, tris(1-phenylpyrazolato,N,C2′)iridium(III) $Ir(ppz)_3$ and Bphen, that effectively confine carriers and excitons and keep them in the EMLs to suppress the colour-shift at different voltages. Ag is used as an anode in the TWOLED. The Sm/Ag bilayer is used as an effective cathode due to a Sm low work function ($\sim$ 2.7 eV), relatively high transparency in the visible range, and Ag environmental stability. Compared with a common Al/Ag cathode, the Sm/Ag cathode has a high transmissivity and a low reflectivity as shown in Fig. 1. We use ZnS as a light outcoupling layer, whose thickness is optimized with the transfer matrix theory.[17] From Fig. 1, we can see that a 24-nm ZnS layer can increase the transmissivity and reduce the reflectivity of the Sm/Ag cathode in the whole visible region. We can obtain a lowest reflectivity (8%) at 492 nm and a mean reflectivity of 24% in the visible area.

TWOLED was grown on a glass substrate. Prior to the device deposition, the substrate was cleaned with acetone and ethanol by using an ultrasonic bath, rinsed with deionized water, and then dried in an oven. All depositions were completed in a high vacuum about 5×10^{-4} Pa. Organic powders were heated to obtain the growth rate of 0.1 nm/s–0.3 nm/s. The current density–voltage–luminance characteristics of the devices were measured with a Keithley 2400 source measurement unit and a Photo-Research PR-655 Spectra Scan Colorimeter in a glove box. All measurements were carried out at room temperature.

Table 1. Structures of all devices.

Device	Structure
A	Ag (70 nm) /MEO-TPD:1.8 wt% F_4-TCNQ (30 nm)/MEO-TPD (10 nm)/CBP:0.5 wt% $Ir(MDQ)_2(acac)$ (5 nm)/SPPO1:10 wt% FIrpic (25 nm)/Bphen (10 nm)/Bphen:Li (20 nm, 1:1 mol)/Sm (8 nm)/Ag (16 nm) /ZnS (24 nm)
B	Ag (70 nm)/MEO-TPD:1.8 wt% F_4-TCNQ (30 nm)/MEO-TPD (10 nm) /$Ir(ppz)_3$ (10 nm)/CBP:0.5 wt% $Ir(MDQ)_2(acac)$ (5 nm)/SPPO1:10 wt% FIrpic (25 nm)/Bphen (10 nm) /Bphen:Li (20 nm, 1:1 mol)/Sm (8 nm)/Ag (16 nm) /ZnS (24 nm)
C	Ag (70 nm)/MEO-TPD:1.8 wt% F_4-TCNQ (30 nm)/MEO-TPD (10 nm)/SPPO1:10 wt% FIrpic (5 nm)/SPPO1 (25 nm)/Bphen (10 nm)/Bphen:Li (20 nm, 1:1 mol)/Sm (8 nm)/Ag (16 nm)
D	Ag (70 nm)/MEO-TPD:1.8 wt% F_4-TCNQ (30 nm)/MEO-TPD (10 nm)/SPPO1 (5 nm)/SPPO1:10 wt% FIrpic (5 nm)/SPPO1 (20 nm)/Bphen (10 nm)/Bphen:Li (20 nm, 1:1 mol)/Sm (8 nm)/Ag (16 nm)
E	Ag (70 nm)/MEO-TPD:1.8 wt% F_4-TCNQ (30 nm)/MEO-TPD (10 nm)/SPPO1 (20 nm)/SPPO1:10 wt% FIrpic (5 nm)/SPPO1 (5 nm)/Bphen (10 nm)/Bphen:Li (20 nm, 1:1 mol)/Sm (8 nm)/Ag (16 nm)
F	Ag (70 nm)/MEO-TPD:1.8 wt% F_4-TCNQ (30 nm)/MEO-TPD (10 nm)/SPPO1 (25 nm)/SPPO1:10 wt% FIrpic (5 nm)/Bphen (10 nm)/Bphen:Li (20 nm, 1:1 mol)/Sm (8 nm)/Ag (16 nm)

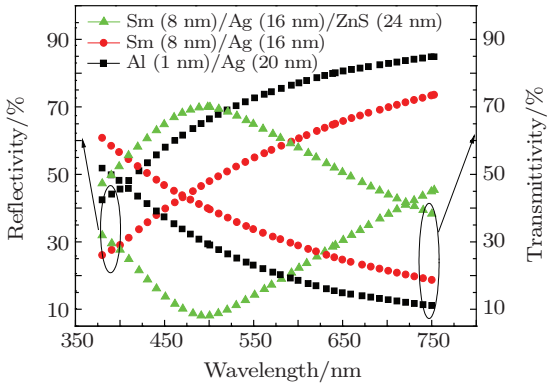


Fig. 1. (colour online) Reflectivity and transmittivity characteristics of the Al (1 nm)/Ag (20 nm) and Sm (8 nm)/Ag (16 nm)/ZnS (0 or 24 nm) cathode.

3. Results and discussion

Although the emitting materials used in device A have a relatively high luminous efficiency, the luminance and efficiency of the whole device is low as shown in Figs. 2(b) and 3 respectively. From the energy level diagram in Fig. 4, we can see that the electron injection from CBP (2.9 eV) into MEO-TPD (2.4 eV) is somewhat more efficient than that from CBP into $Ir(ppz)_3$ (1.6 eV). Therefore, holes and electrons are confined inside the red and blue emitting layers and a low current density is observed in device B (Fig. 2(a)). The leakage current in device A is higher than that in device B (Fig. 2(a)), indicating that the p–i–n structure in device A is not good enough for charge confinement, especially in preventing the electrons injection into HTL. Compared with device A, device B exhibits a low current density and a low leakage current as shown in Fig. 2, but a high luminance, indicating the insertion of a $Ir(ppz)_3$ layer which effectively blocks the electron from injecting into the HTL and further into the anode. It can be obviously seen in Fig. 2(b) that the maximum brightness increases from 2195 cd/m^2 to 3861 cd/m^2 at 13 V. The maximum brightnesses of both devices are low due to a relatively thick Sm, whose light absorption is serious, resulting in the low brightness. If a thicker Ag and a thinner Sm are used, the microcavity effects in the devices will become serious and it is hard to obtain a white emission. The maximum current efficiency of device B is 9.8 cd/A at 8 V and the maximum power

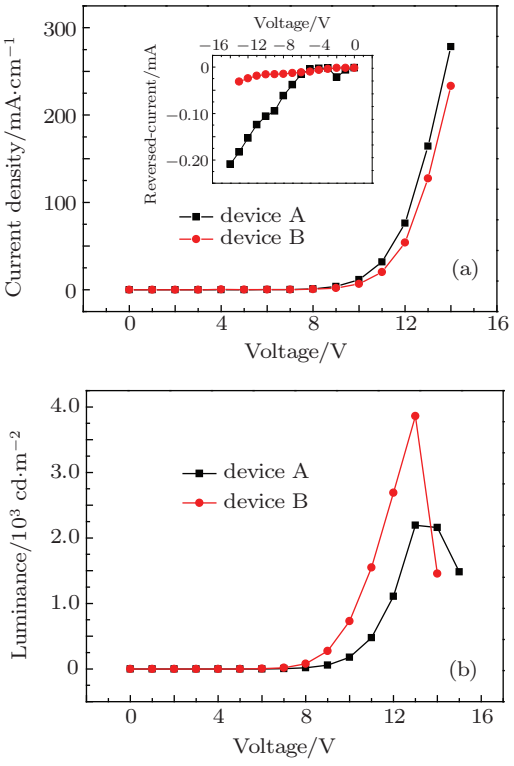


Fig. 2. (colour online) Current density–voltage (a) and luminance–voltage (b) characteristics of devices A and B. Inset shows the leakage current–voltage characteristics.

efficiency is 4.2 lm/W at 7 V, while the maximum efficiencies of device A are 2.7 cd/A at 10 V and 0.91 lm/W at 9 V as shown in Fig. 3.

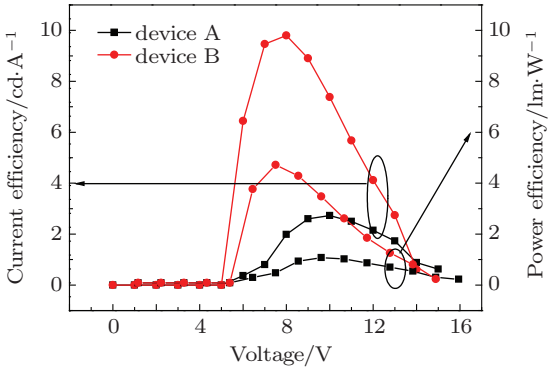


Fig. 3. (colour online) Variations of current efficiency and power efficiency with drive voltage for devices A and B.

Figure 5 shows the normalized EL spectra of the devices under different driving voltages. Obviously, no significant EL spectrum change can be observed in device B as the driving voltage increases from 6 V to 11 V. The corresponding CIE coordinates in device B are (0.4528, 0.4519) at 6 V and (0.4352, 0.4612) at 11 V, and the variation of (±0.0088, ±0.0046) is much less than those observed by the human eye, indicating that device B demonstrates here an excellent colour stability. Figure 6 shows the EL spectra of device B normalized to 592 nm at viewing angles from 0° to 75° at a voltage of 11 V. The CIE$_{x,y}$ coordinates measured at 11 V change from (0.4511, 0.4593) to (0.4562, 0.4578) at viewing angles from 0° to 45°, corresponding to a variation of (±0.0025, ±0.0008), whose change is far smaller than those of other TWOLEDs reported in Refs. [18]–[21]. Even at a viewing angle of 75°, the CIE$_{x,y}$ coordinates are changed by values that are as small as (±0.0087, ±0.0013). The very weak angular dependence in the spectrum also indicates a very weak microcavity effect.

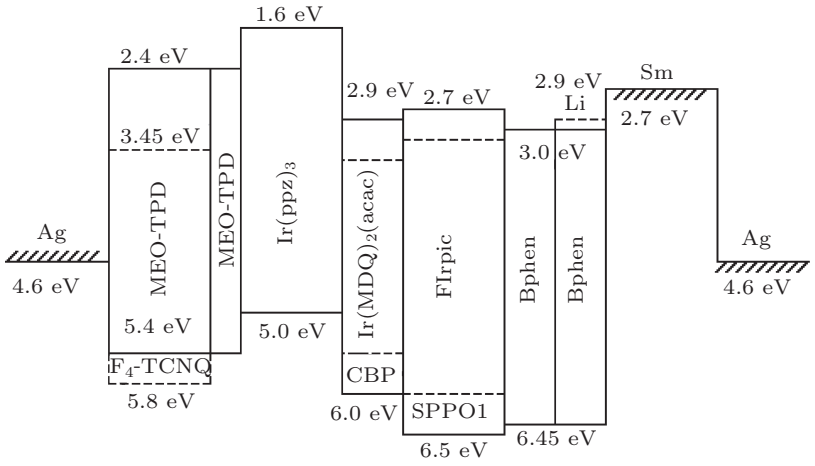


Fig. 4. Energy level diagram of the used materials in device B.

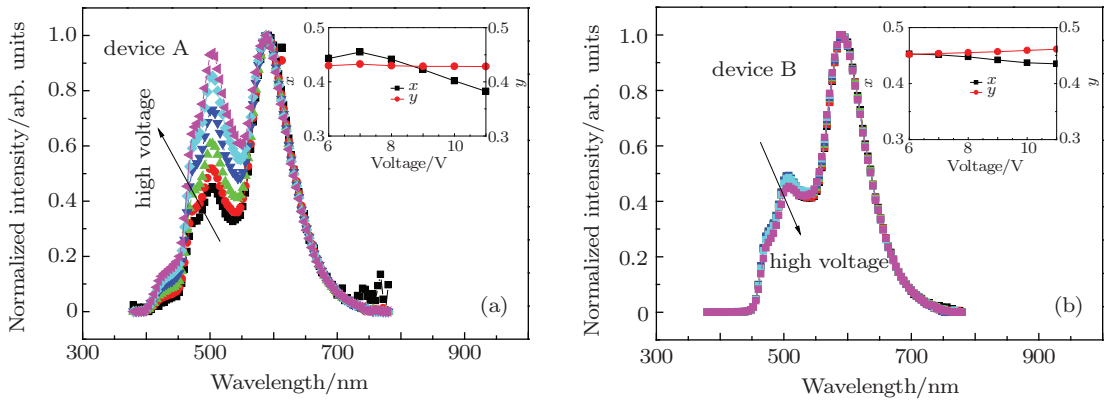


Fig. 5. Variations of EL spectra with voltages for devices A (a) and B (b). Insets show x, y indexes of colour coordinates.

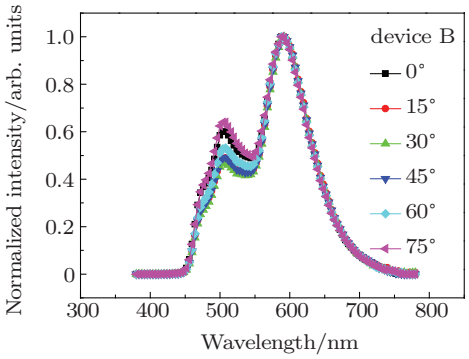


Fig. 6. (colour online) Angular dependences of EL spectra of device B at a voltage of 11 V at viewing angles from 0° to 75°.

It is universally received that the colour stability of the WOLED could be influenced by some factors, such as, carrier trapping, exciton recombination zone, etc. To clarify the electron blocking effect induced by the $Ir(ppz)_3$ layer and observe the main recombination area, single-emitting layer devices named devices C, D, E, and F with the FIrpic emitter located at different places in the SPPO1 host are designed, whose structures are shown in Table 1. The absolute EL spectra of these devices at various current densities are shown in Fig. 7. It can be found that there is an emission peak at approximately 428 nm, indicating that the hole transport layer MEO-TPD is also emitting, whose photoluminescence peak is at 429 nm. However, device B effectively prevents the MEO-TPD from emitting as shown in Fig. 5(b), owing to the insertion of an $Ir(ppz)_3$ layer and its electron blocking effect. At a low current density of 5 mA/cm^2, device C has the highest blue emission peak at 472 nm with a value of 1.75×10^{-4}, while device F has a peak value of 5.94×10^{-5}, which reveals that the main exciton recombination zone is at the MEO-TPD/SPPO1 interface in the low voltage case. The reason for this is that the holes are difficult to overcome with a total barrier of 1.1 eV of the MEO-TPD/SPPO1 interface at a low voltage. As the driving voltage increases gradually, the external electric field offers enough energy, which makes the holes inject from MEO-TPD into SPPO1 more easily. So the main exciton recombination zone changes to the SPPO1/Bphen interface. For example, at a current density of 100 mA/cm^2, the values of the highest emission peaks in devices C, D, E, and F are 0.00323 (at 500 nm), 0.00232 (at 472 nm), 0.00263 (at 472 nm) and 0.0041 (at 500 nm), while those of blue emission peaks (at 472 nm) are 0.0028, 0.00232, 0.00263 and 0.00375 respectively. All these results indicate that the main exciton recombination zone is at the SPPO1/Bphen interface for the case of the high electric field. Although

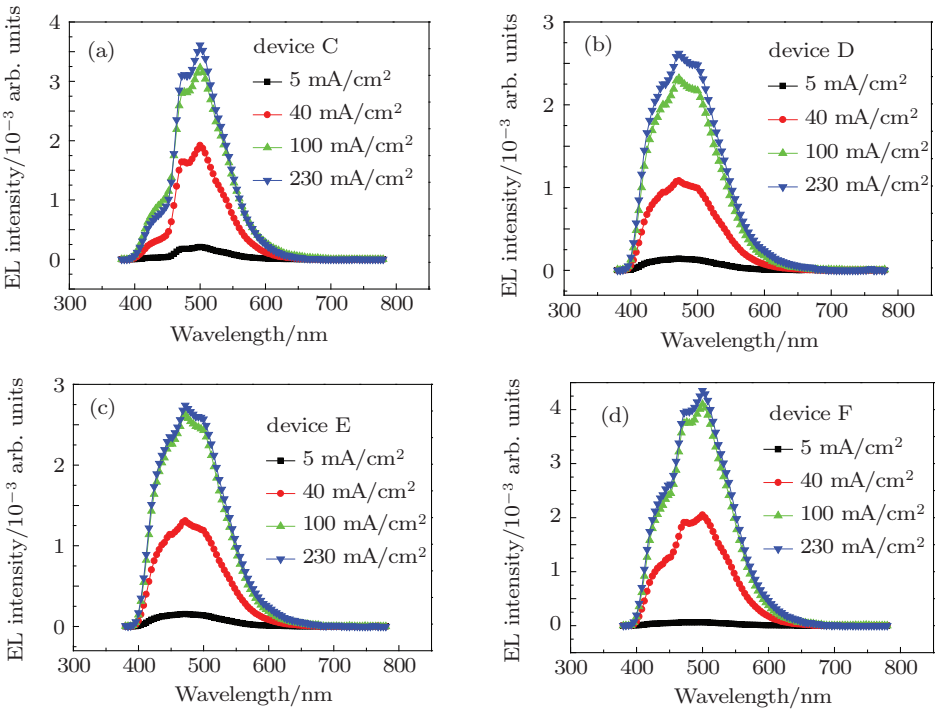


Fig. 7. (colour online) EL spectra of the devices C (a), D (b), E (c), and F (d) at current densities of 5, 40, 100, and 230 mA/cm^2.

the MEO-TPD/SPPO1 interface is also the main exciton recombination zone, the number of exciton recombination is less than that at the SPPO1/Bphen interface. Of the two interfaces, there is a combination of a relatively small number of excitons in SPPO1, which also indicates that SPPO1 is a good bipolar transport material. The insertion of an $Ir(ppz)_3$ layer in device B restricts the exciton recombination zone mainly into the CBP and SPPO1 layers. In device B, the main exciton recombination zone is in the red layer and the blue layer close to the red region at a low voltage. At a high voltage, the main exciton recombination zone should change to the blue region and so the blue luminous intensity should increase, but we find it in fact reduces in Fig. 5(b). The reason for this is that electrons inject from SPPO1 into CBP without any energy barrier while the holes inject from CBP into SPPO1 with an energy barrier of 0.5 eV. Therefore, the main exciton recombination zone in device B is confined into CBP. SPPO1, with good hole transport characteristics makes the luminous intensity ratio of blue to red maintain almost no change, which is a key factor of the good colour stability.

4. Conclusions

In this paper, we demonstrated a top-emitting electrophosphorescent p–i–n WOLED on the basis of a low-reflectivity Sm/Ag semi-transparent cathode together with a thickness-optimized ZnS outcoupling layer. When an efficient electron blocking layer $Ir(ppz)_3$ is introduced into the top emitting WOLED to confine the exciton recombination area, not only the brightness and the luminous efficiency can be significantly enhanced due to the reduced leakage current and efficient recombination of excitons in the emissive area, but also an extremely stable EL spectrum is obtained both in a large EL intensity range and at a large viewing angle. The main reasons for this are analysed in detail. The highly efficient TWOLED with excellent chromaticity stability has a wide application in flat-panel displays and lighting.

References

[1] Jiao Z Q, Wu X M, Hua Y L, Dong M S, Su Y J, Shen L Y and Yin S G 2011 *Chin. Phys.* B **20** 107803

[2] Yang Y, Chen S F, Xie J, Chen C Y, Shao M, Guo X and Huang W 2011 *Acta Phys. Sin.* **60** 047809 (in Chinese)

[3] Cao G H, Qin D S, Guan M, Cao J S, Zeng Y P and Li J M 2008 *Chin. Phys.* B **17** 1911

[4] Chen S F, Shao M, Guo X, Qian Y, Shi N E, Xie L H, Yang Y and Huang W 2012 *Acta Phys. Sin.* **61** 087801 (in Chinese)

[5] Ko Y W, Chung C H, Lee J H, Kim Y H, Sohn C Y, Kim B C, Hwang C S, Song Y H, Lim J, Ahn Y J, Kang G W, Lee N and Lee C 2003 *Thin Solid Films* **426** 246

[6] Attar H A A, Monkman A P, Tavasli M, Bettington S and Bryce M R 2005 *Appl. Phys. Lett.* **86** 121101

[7] Zhang L J, Hua Y L, Wu X M, Wang Y and Yin S G 2008 *Chin. Phys.* B **17** 3097

[8] Jiang X Y, Zhang Z L, Zhang B X, Zhu W Q and Xu S H 2002 *Synth. Met.* **129** 9

[9] Chuen C H, Tao Y T, Wu F I and Shu C F 2004 *Appl. Phys. Lett.* **85** 4609

[10] Shao Y and Yang Y 2005 *Appl. Phys. Lett.* **86** 73510

[11] Wang Y Z, Sun R G, Meghdadi F, Leising G and Epstein A J 1999 *Appl. Phys. Lett.* **74** 3613

[12] Wu Y S, Hwang S W, Chen H H, Lee M T, Shen W J and Chen C H 2005 *Thin Solid Films* **488** 265

[13] Sun Y, Giebink N C, Kanno H, Ma B, Thompson M E and Forrest S R 2006 *Nature* **440** 908

[14] Gong X, Wang S, Moses D, Bazan G C and Heeger A J 2005 *Adv. Mater.* **17** 2053

[15] Chen S F, Deng L L, Xie J, Peng L, Xie L H, Fan Q L and Huang W 2010 *Adv. Mater.* **22** 5227

[16] Jeon S O, Yook K S, Joo C W, Son H S and Lee J Y 2010 *Thin Solid Films* **518** 3716

[17] Chen S F, Xie W F, Meng Y L, Chen P, Zhao Y and Liu S Y 2008 *J. Appl. Phys.* **103** 054506

[18] Kanno H S, Sun Y R and Forrest S R 2005 *Appl. Phys. Lett.* **86** 263502

[19] Chen S M and Kwok H S 2011 *Org. Electron.* **12** 677

[20] Ma J, Piao X C, Liu J, Zhang L T, Zhang T Y, Liu M, Li T, Xie W F and Cui H N 2011 *Org. Electron.* **13** 1187

[21] Ji W Y, Zhang L T, Zhang T Y, Xie W F and Zhang H Z 2010 *Org. Electron.* **11** 202